New seismic data improve earthquake location in the Vienna Basin area, Austria

Helmut HAUSMANN[1)*)], Stefan HOYER[2)], Bernd SCHURR[2)3)], Ewald BRÜCKL[1)], Gregory HOUSEMAN[4)] & G. STUART[4)]

[1)] Institute of Geodesy and Geophysics, Vienna University of Technology, Gusshausstrasse 27-29/1282, A-1040 Vienna, Austria;

[2)] Department of Meteorology und Geophysics, University of Vienna, Althanstrasse 14, A-1090 Vienna, Austria;

[3)] Department of Geodynamics, Helmholtz-Zentrum Potsdam, Deutsches GeoForschungsZentrum GFZ, Telegrafenberg, C 223, D-14473 Potsdam, Germany;

[4)] Faculty of Earth and Environment, University of Leeds, Leeds, LS2 9JT, UK;

[*)] Corresponding author, hausmann@mail.zserv.tuwien.ac.at

Abstract

The area extending from the upper Mürz Valley to Semmering, and on to the southern Vienna Basin, belongs to the seismically most active regions in Austria. Because of the population density and sensitive infrastructure, seismic hazard assessment is an important issue. Routine location of earthquakes carried out by the Central Institute for Meteorology and Geodynamics, Austria, images well the general seismicity pattern. However, a correlation with individual faults cannot be resolved. In this study, recordings from passive seismic monitoring projects (ALPASS and CBP) and permanent seismic network data are used together with a new 3D seismic velocity model to locate earthquake hypocentres in the Vienna Basin area. Three different location methods were applied. Focal coordinates of the 44 earthquakes determined by these methods depend on the applied method and differ considerably from the routine locations. Analysis of the residual travel-times and the location of quarry blasts showed that the best results were achieved with a probabilistic location method based on the new 3D velocity model for P- and S waves. An absolute accuracy of ~3 km was obtained by this method. Clustering and linear alignment of epicentres as well as their probability density functions allow for the correlation with local fault systems. Hypocentres with increasing focal depth closely follow the Mur-Mürz in the Semmering area and its extension to the Pottendorf fault in the southern Vienna Basin. Further, the continuation of the Salzach-Ennstal-Mariazell-Puchberg fault towards the Vienna Basin has been imaged clearly by epicentres. Implementation and further improvement of the 3D velocity model has the potential to enhance accuracy of routine epicentre location.

Das Gebiet zwischen dem oberen Mürztal über den Semmering bis hin zum südlichen Wiener Becken gehört zu den seismisch aktivsten Regionen in Österreich. Aufgrund der hohen Bevölkerungsdichte und sensitiver Infrastruktur ist die seismische Risikobewertung ein wichtiges Thema. Routinemäßige Lokalisierungen der Zentralanstalt für Meteorologie und Geodynamik (ZAMG) bilden das generelle Seismizitätsmuster ab. Eine Korrelation mit einzelnen Störungen kann nicht aufgelöst werden. In dieser Arbeit werden Aufzeichnungen von temporären seismischen Monitoring Projekten (ALPASS und CBP) und Daten permanenter seismischer Netzwerke, sowie ein neues 3D Modell der seismischen Geschwindigkeiten verwendet um Erdbeben im Bereich des südlichen Wiener Beckens zu lokalisieren. Zur Berechnung der Herdkoordinaten von 44 Erdbeben wurden 3 verschiedene Methoden angewandt. Die Ergebnisse unterscheiden sich beträchtlich von den Routineauswertungen. Die Evaluierung von Laufzeitresiduen sowie die Anwendung der Methoden auf Ortungen von Sprengungen in Steinbrüchen mit bekannter Lage zeigten, daß die lokalisierten Epizentren sich mit einem wahrscheinlichkeitstheoretischen Ansatz in Kombination mit dem 3D-Geschwindigkeitsmodell für P- und S Wellen am besten abbildeten. Mit dieser Methode konnte eine absolute Genauigkeit von ~3 km erreicht werden. Die Lage der Epizentren sowie die Verteilung der Wahrscheinlichkeitsdichtefunktion ermöglicht eine Korrelation mit lokalen Störungssystemen. Hypozentren mit zunehmender Herdtiefe folgen der Mur-Mürz über den Semmering hin bis zur Pottendorfer Störung im südlichen Wiener Becken. Weiters konnte der Verlauf der Salzach-Ennstal-Mariazell-Puchberg Störung zum Wiener Becken hin durch die Lage einiger Epizentren abgebildet werden. Die Implementierung und weitere Verbesserung des 3D Geschwindigkeitsmodells in die routinemäßige Bestimmung der Hypozentren wird zu einer wesentlichen Steigerung der Genauigkeit führen.

1. Introduction

The southern Vienna Basin and the Mur-Mürz Valley are the seismically most active regions in Austria (Hammerl and Lenhardt, 1997). Since 1201, fourteen earthquakes with macroseismic intensities > 7 (EMS) have been recorded in this area. The earthquake in the wider area of Neulengbach in 1590, about 30 km east of Vienna, had an epicentral intensity of about 9, according to the analysis of historical documents (Lenhardt et al., 2007). Most other earthquakes cluster around the Mur-Mürz fault (MM) and the Vienna Basin Transfer fault (VBT) (Fig. 1).

This region, including the capital Vienna, has more than 2 million inhabitants and sensitive infrastructure. Seismic hazard assessment and mitigation is therefore an important task. Especially for the city of Vienna, an estimate of the maximum plausible earthquake is relevant, but still an open question. For example, Hinsch and Decker (2003) determined the seismic slip deficits for various sectors of the VBT. The authors estimated that a high intensity earthquake of a minimum magnitude of M = 6.1 (about every 800 years) is necessary to pro-

duce the geologically estimated slip for the Lassee segment of the VBT.

Basic data for seismic hazard assessment and seismogenic processes are accurate earthquake hypocentres and their spatial relation to tectonic faults. Such data support the identification of seismo-tectonically active faults. Magnitude and focal mechanism provide further information on stress release and the kinematics of faults. Only two seismic observatories (CONA and SOP) are located within a distance of 50 km from faults in the southern Vienna Basin (Fig. 2). However, in any case the low number of seismic stations near the area of interest limits the accuracy of locating earthquakes, which is routinely carried out by the Central Institute for Meteorology and Geodynamics, Austria (ZAMG). Another limitation on accuracy is the restriction to the 1D velocity model IASP91. The large lateral velocity variations, particularly due to the geological structures of the Vienna Basin, deviate significantly from a 1D model.

Data from recent passive- and controlled-source seismic experiments covering the Vienna Basin area offer the opportunity to overcome the limitations addressed before and to improve the accuracy of earthquake location. From May 2005 to August 2007, seismic data were collected during the passive seismic monitoring projects ALPASS (Brückl et al., 2008) and CBP (Houseman et al., 2008). This data, together with recordings from up to 10 permanent seismic observatories are used to relocate earthquakes in the Vienna Basin and the upper Mürz Valley. Improved velocity information, especially 3D P-wave and S-wave velocity models and a new map of the Moho discontinuity (Behm et al., 2007; Behm 2009) derived from CELEBRATION 2000 (Guterch et al., 2003) and ALP 2002 (Brückl et al., 2003), as well as controlled-source seismic data are implemented into earthquake location in this region. The effect of an increased number of stations and the refined velocity information on the accuracy of earthquake location is analyzed using recordings of large quarry blasts with known locations. Finally, we provide a preliminary correlation of the new earthquake locations with known geological structures and discuss their impact on an improved tectonic interpretation. Our investigation is a pilot study with respect to ongoing efforts to increase the resolution of seismic data in the Mur-Mürz and Vienna Basin area.

2. Active tectonics

The collision of the European and Adriatic plates, the exhumation of the Penninic windows, together with the eastward extrusion of crustal blocks into the Pannonian basin, have been the primary tectonic processes to shape the Eastern Alps and to imprint the fault systems controlling present day crustal dynamics. The most active tectonic structures in the study area are the Mur-Mürz fault (MM) and its continuation, to the NE, the Vienna Basin Transfer fault (VBT) (Fig. 1). Strike-slip along these faults is sinistral and follows the kinematics of ongoing extrusion of crustal blocks from the Eastern Alps to the Pannonian Basin (Ratschbacher et al. 1991; Peresson and Decker, 1997; Linzer et al., 1997; 2002). High seismicity and offset Quaternary sediments show ongoing fault activity along MM and VBT (Aric and Gutdeutsch, 1981; Gutdeutsch and Aric, 1988; Decker and Peresson, 1998; Hinsch et al., 2005a, 2005b). Hypocentres have been located between 4 and 8 km focal depth. Stress estimates and focal mechanisms follow mainly sinistral strike-slip in the fault direction (Gangl, 1975; Gutdeutsch and Aric 1988; Marsch et al., 1990; Reinecker and Lenhardt, 1999; Decker et al., 2005; Decker and Burmester, 2008). However, regional moment tensor solutions from the Swiss Seismological Service indicate that normal faulting also occurs in the southern Vienna Basin (SED, 2000).

The VBT crosses the Vienna Basin (VB) near its south-eastern border. The VB is a thin-skinned subsiding pull-apart basin which developed in the Miocene (Royden 1993; Decker,
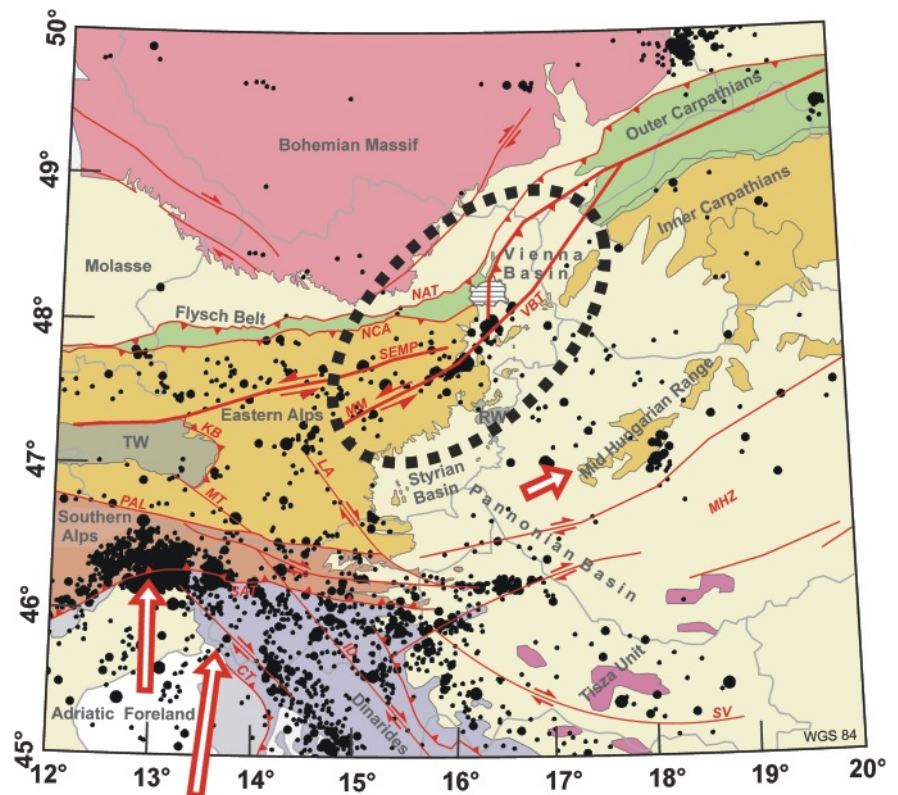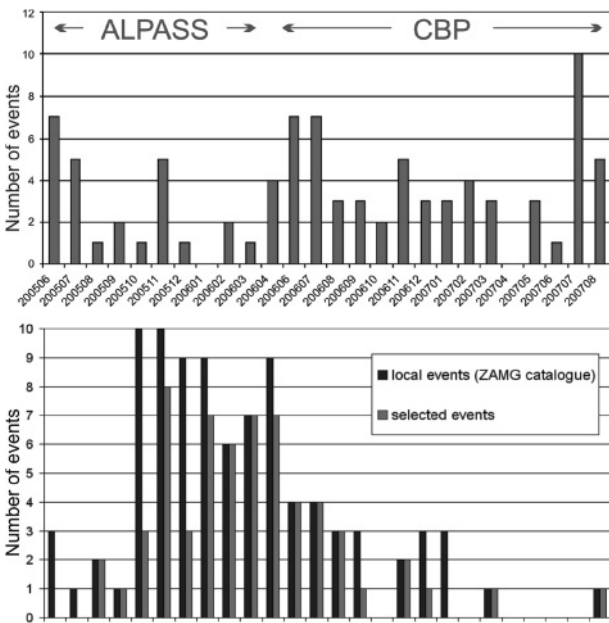

Figure 1: Major geological units and tectonic structures of the Eastern Alps (after Oberhauser, 1980; Schmid et al., 2004). Seismic activity is shown by earthquakes epicentres (black circles) extracted from the NEIC catalogue (1973-2008). The study area is enclosed by a dotted ellipse; LA (Lavanttal fault), MM (Mur-Mürz fault), NAT (North Alpine Thrust), NCA (Northern Calcareous Alps Thrust), PAL (Periadriatic Line), SEMP (Salzach-Ennstal-Mariazell-Puchberg fault), VBT (Vienna Basin Transfer Fault), RW (Tauern and Rechnitz window), extent of Vienna is marked by horizontal hatches.
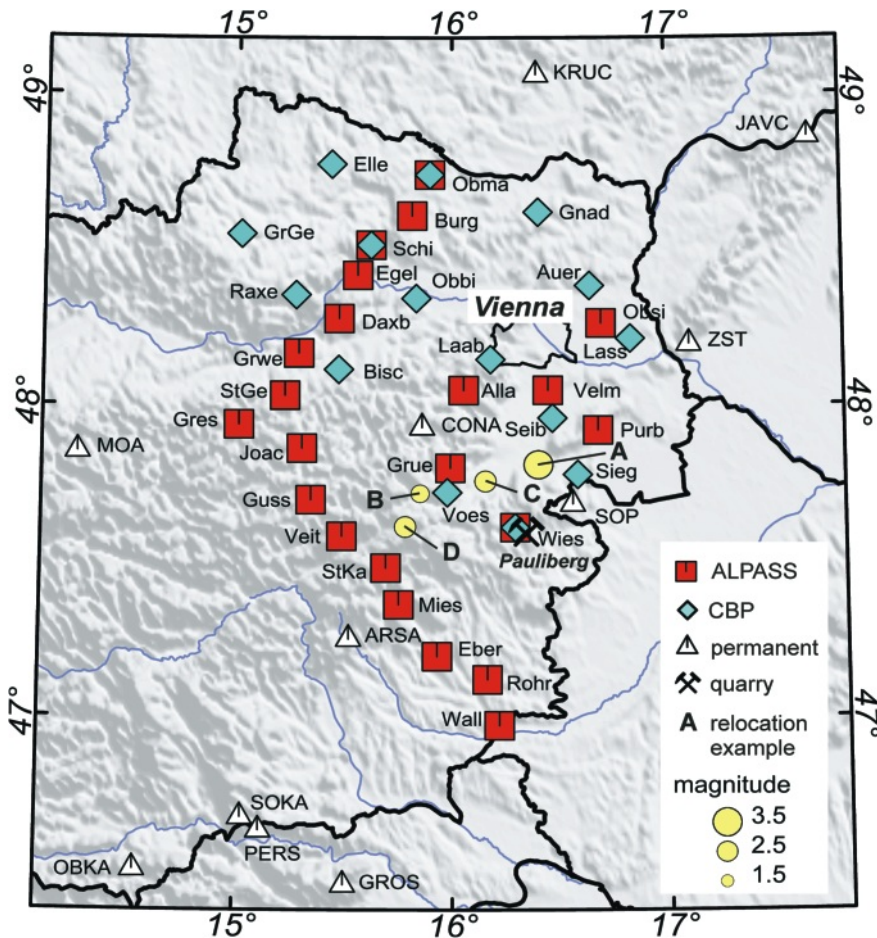
Figure 2: Location of temporal (ALPASS and CBP) and permanent seismic stations used for this study. Characters A, B, C, and D identify epicentres of earthquakes which were analyzed to find the best location method. The quarry Pauliberg used for validation of the absolute location accuracy is also shown in this map.

Figure 3: Seismicity of the investigation area for the monitoring period from June 2005 – August 2007, extracted from the bulletin of the Austrian Seismological Service (ZAMG): (a) Monthly number of local events; (b) Distribution of the local magnitude (Ml) divided in events detected within the study area and events selected for the relocation.

1996; Decker and Peresson, 1998). Historical documented and instrumentally recorded seismicity declines significantly to the central and north-eastern parts of the VB. However, an analysis of data on the historical Carnuntum earthquake around 350 A.D. demonstrates that the possibility of an I ~ 9 (Ml ~ 6) earthquake should be taken into consideration even in this part of the VB (Decker et al., 2006).

Another structure highly active during lateral extrusion is the Salzach-Enns-Mariazell-Puchberg fault (SE-MP), where sinistral displacements up to 60 km were geologically determined since the Early Miocene (e.g. Linzer et al., 2002). Seismic activity at the SEMP is significantly lower than at the MM and VBT. The region near the Northern Floor Thrust of the Eastern Alps and the front of the Northern Calcareous Alps appears currently seismically inactive. But one should keep in mind that the largest earthquake in Austria, Neulengbach 1590, occurred in this wider area. Since the location of the epicentre is not well constrained by the historical documents (Gutdeutsch et al., 1987, Hammerl and Lehnhardt, 1997) it could also have been placed in the VB.

Precise levelling surveys (Senftl and Exner, 1973; Höggerl, 1989; Vyskocil, 1994) show that the southern Vienna Basin is subsiding relative to the Austrian First Order Levelling Network reference point, located near Horn in the Bohemian Massif. Subsidence is related to a sinistral strike-slip pullapart mechanism, with 1.5- to 2 km slip determined during the Quaternary (Decker and Peresson, 1998; Decker et al., 2005; Hinsch et al., 2005b). GPS-derived crustal velocities suggest a current relative displacement rate of 1 - 2 mm/yr for the VBT (Grenerczy et al., 2006, 2009; Haslinger et al., 2007). Spatial resolution of this data is not sufficient to determine displacement rates along the individual faults in our area of interest.

3. Seismic networks and data

3.1 Temporary networks

Data from the temporary networks ALPASS and CBP cover a period of 27 months from 2005 - 2007 with an average interstation distance of about 50 km (Fig. 2). In the ALPASS project, 17 of the selected stations were located along two approximately perpendicular profiles (NE-SW and NW-SE), 5 other stations group in and around the Vienna Basin (Fig. 2). The

4

station network consisted of short-period instruments which re-corded data from May 12th, 2005, to May 4th, 2006, at sample rates of 40 and 50 sps. Most of these stations were installed in cellars of buildings with firm foundations. The 15 Austrian CBP stations were broadband sensors (30 s natural periods Guralp CMG 6TD), mainly installed outdoors along three parallel SE oriented profiles. The CBP data were sampled with 100 sps and recorded from April 4th, 2006, to August 20th, 2007.

3.2 Permanent networks

Broadband data from permanent seismic networks are also included in our analysis. Event broadband waveforms were kindly provided by the Austrian Seismic Network (A) and the Seismological Station Net-work in Hungary (HU) for the sta-tions CONA (A), ARSA (A) and SOP (HU). In addition, perti-nent day volumes were collected for the stations ZST (SK), JAVC (CZ), KRUC (CZ), VRAC (CZ), and MOA (A), OBKA (A) via ORFEUS (Observatories and Research Facilities for Euro-pean Seismology).

3.3 Selected seismic events

The detection and location of local earthquakes and quarry blasts within Austria is routinely carried out by ZAMG. Figure 3a shows the number of events per month, which were loca-ted in the Vienna Basin and the upper Mürz Valley. The events are characterized by local magnitudes (determined by ZAMG) between Ml = 1 and about 2.8 with one larger event of Ml = 3.5 on 2005.07.25 03:06. During the ALPASS deployment (19.5. 2005 – 4.5.2006), 41 local events were detected in the Vienna Basin with local magnitudes between 1.1 and 3.5. For the du-ration of the CBP project (10.4.2006 – 22.8. 2007), 75 local events were detected with magnitudes between 1.0 and 2.8. Eleven quarry blasts from Pauliberg (for location, see Fig. 2) were well recorded by these temporary networks. For this stu-dy, 20 events from the ALPASS data set (1.2 < Ml < 3.5) and 24 events from the CBP data set (1.5 < Ml < 2.8) were selec-ted for relocation (Fig. 3b). The ALPASS dataset was resam-pled to 80 sps and, together with the CBP data, trimmed to
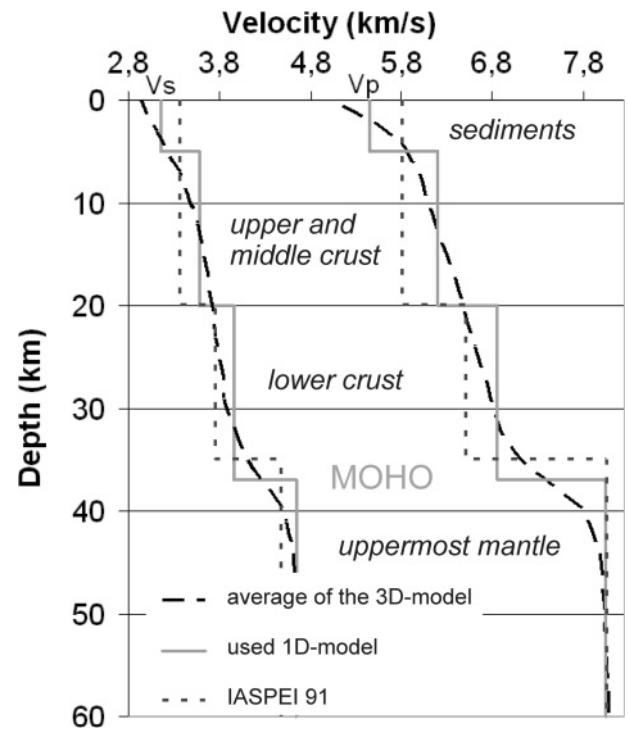

Figure 4: The 1D constant layer model for P- and S-waves, the IASPEI 1991 model and the average 1D-model derived from the 3D-model of the crust of the Eastern Alps (Behm et al., 2007).

event-windows using the software "Seismon" (Mertl and Haus-mann, 2009; http://sourceforge.net/projects/seismon) before picking arrivals.

4. Location methods

Standard single earthquake location programs such as HYPO 71 (Lee and Jahr, 1975), HYPOINVERSE (Klein, 2002) and HYPOELLIPSE (Lahr, 1999) are limited to 1D velocity models (layered) for travel-time calculation. For complex 3D structu-res, the implementation of 3D velocity models into the loca-tion method is an advantage. Lomax et al. (2000) described a probabilistic earthquake location method, which can be applied for 1D- as well as complex 3D-velocity models. Further im-
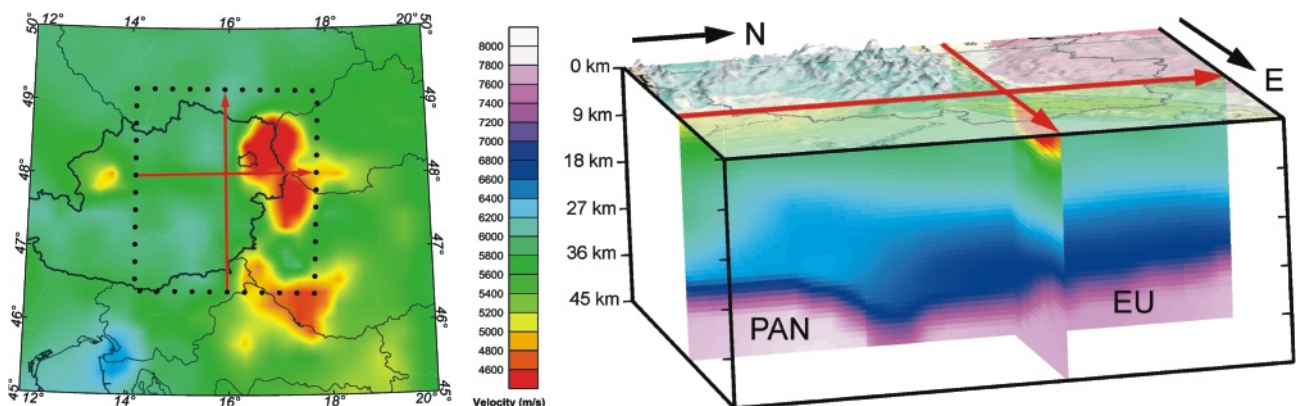
Figure 5: Visualization of the 3D seismic P-wave velocity model of the Eastern Alps (Behm et al., 2007). (a) Depth slice at 3 km depth below N.N; the dotted rectangle marks the extent of the velocity model we used in this study, red arrows mark the location of the cross sections shown in (b) the EW directed section displays the area from the Molasse zone across the Vienna Basin to the Pannonian Basin. The NS directed section displays the area from the Bohemian massive across the Eastern Alps to the Styrian Basin. EU (European plate), PAN (Pannonian fragment).

Methods	Mean horizontal distance	Max. horizontal distance
NonLinLoc 3D – NonLinLoc 1D	1.4 ± 0.6 km	2.2
NonLinLoc 3D – Hypo 71	1.4 ± 0.7 km	2.3
NonLinLoc 3D – ZAMG	4.3 ± 3.5 km	9.5
NonLinLoc 1D – Hypo 71	1.4 ± 0.5 km	2.1
NonLinLoc 1D – ZAMG	3.7 ± 3.3 km	8.5
Hypo 71 - ZAMG	3.1 ± 4.2 km	9.0

TABLE 1: Relative comparison of the 44 epicentre locations calculated by either this study or the ZAMG. Each row shows the mean horizontal distance for two location methods.

provement of locations relative to master events or a group of events could be achieved by the double-difference method (Waldhauser and Ellsworth, 2000) or the Joint Event Location – JHD technique (Pujol, 1995). However, in this study we are interested in high absolute location accuracy, as we want to relate hypocentre locations to tectonic faults. Therefore, we restrict our study to the evaluation of single events applying the procedures described below.

4.1 Travel-time picking

First arrival P- and S-wave signals were picked manually using PITSA, part of the GIANT software package (Rietbrock and Scherbaum, 1998). For a hypocentre close to the surface, a representative cross-over distance for Pn arrivals of about

170 km was found from controlled-source seismograms on the CEL10/Alp04 profile from the CELEBRATION 2000 and ALP 2002 experiments (Grad et al., 2009). Epicentres coordinates from the ZAMG bulletin, or obtained from a preliminary evaluation of our data, are used to transform horizontal components into the radial and transverse components. P-wave arrivals were picked from the Z-component; S-wave arrivals from the transverse component. Filtering with a zero-phase Butterworth band pass filter (1 – 10 Hz) or integration was applied, in case enhancement of the signal-to-noise ratio was an issue. Uncertainties in travel time picking of either P- or S-arrivals was considered by weighting functions. We defined 5 classes between the limits 0, 0.1, 0.3, 0.5, 0.75 and 1.00 s. 669 P- and 580 S-wave first arrival travel-times were determined by this procedure. The best signal-to-noise ratio was provided by stations located on the Bohemian Massif or the Eastern Alps (Austroalpine Basement and Northern Calcareous Alps). Signals with low signal-to-noise ratio were recorded in the Molasse zone, the Vienna Basin and the Styrian Basin.

4.2 Location using a local 1D velocity model

As a standard earthquake location routine we used the linearized algorithm of Hypo71 (Lee and Lahr, 1975) in combination with a 1D velocity model. In Hypo71 the hypocenter is found iteratively by least square inversion using Geiger's method (Geiger, 1912) to minimize the root-mean-square (RMS) of the travel-time residuals.

The 1D P-wave velocity (Vp) model (Fig. 4) has four layers: a near-surface layer (Vp 5.45 km/s), an upper and middle crust (Vp 6.20 km/s), a lower crust (Vp 6.85 km/s) and the uppermost mantle (8.04 km/s). The velocities were averaged from the 3D-model of the crust for the Eastern Alps determined by Behm et al. (2007). The depth to the Moho is 37 km. The average Vp/Vs from Behm's (2009) analysis is 1.75, whereas a Wadati diagram of the observed data indicates a value of 1.71 ± 0.05. Thus, we decided to use the well-established value of 1.73. The 1D-model used by the ZAMG (IASPEI 1991) is also shown in Figure 4.
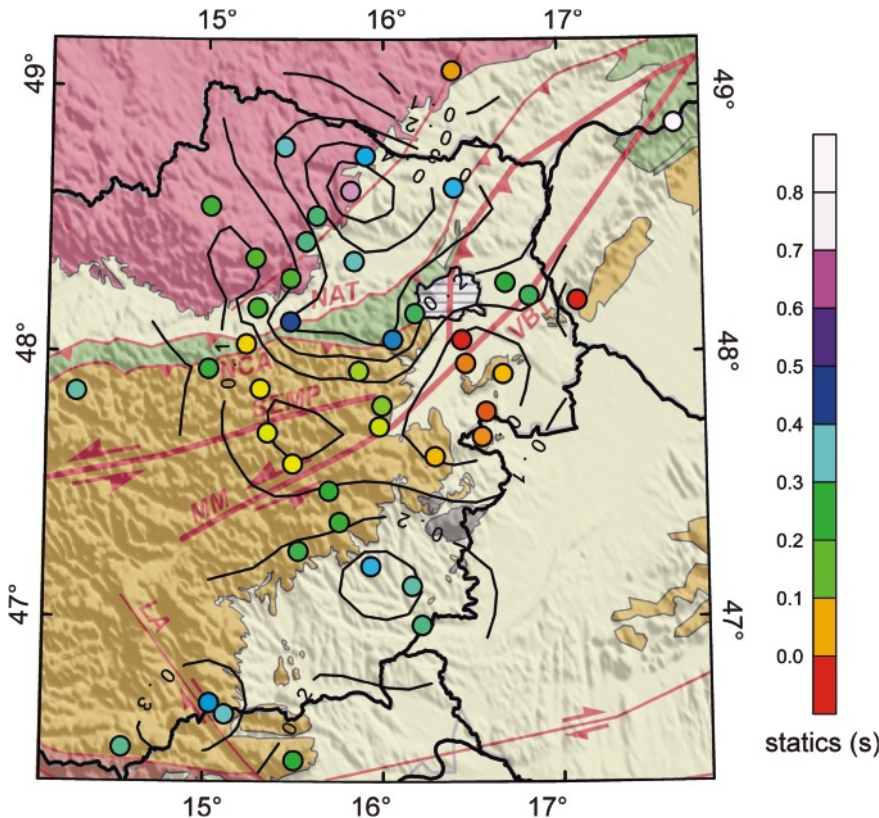
FIGURE 6: Preliminary station corrections for P-wave times for the 3D velocity model displayed as contour lines and symbols (coloured circles) over the major geological and tectonic structures of the Eastern Alps. LA (Lavanttal fault), NAT (North Alpine Thrust), NCA (Northern Calcareous Alps Thrust), MM (Mur-Mürz fault), SEMP (Salzach-Ennstal-Mariazell-Puchberg fault).

4.3 Location using a 3D velocity model

For hypocenter relocation with the 3D velocity model, we use the probabilistic nonlinear earthquake location method of the software package NonLinLoc (Lomax et al., 2000). The location algorithm follows the probabilistic formulation of inversion presented by Tarantola and Valette (1982). The NonLinLoc program produces a misfit function, optimal hypocenters, and an estimate of the posterior probability density function (PDF) for the hypocenter location, using either a systematic grid search or a stochastic, Metropolis-Gibbs sampling approach. To make the location program efficient for complicated 3D-models, the travel-times between each station and all grid nodes are calculated once using a 3D version of the Eikonal finite-difference scheme of Podvin and Lecomte (1991). For this study, the estimated maximum likelihood of the hypocenter and the complete PDF was obtained by the grid search algorithm, which detects multiple minima in the PDF. The 3D-model for the Eastern Alps resulted from active source experiments (Behm et al., 2007; Behm, 2009) and provides P- and S- wave velocities on a 3D grid with a lateral X/Y-spacing of 20/30 km. The vertical grid spacing is variable. For both P- and S-wave velocities a local 271 x 307 x 67 km wide 3D-model, interpolated linearly from the original model onto a 1 km grid, was generated. Visualizations of the interpolated 3D-model are shown in Figure 5, including the Moho at depths between 30 and 45 km. The depth slice at Z = 3 km through the original P-wave velocity model (Fig. 5a) shows low velocities in the VB and Pannonian Basin. In Figure 5b two cross sections through the local velocity model from Z = 0 to Z = 45 km are shown. The EW section displays the area from the Molasse Zone across the VB to the Pannonian Basin and clearly reflects the
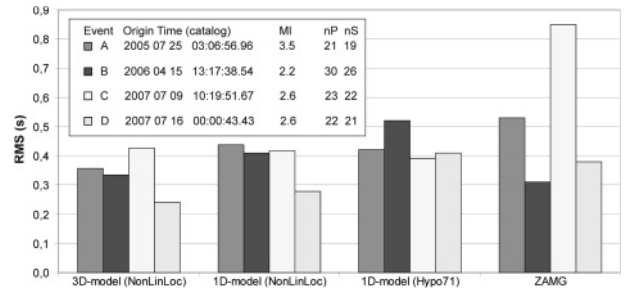

Figure 8: RMS error for travel-time residuals of the four selected events from the three locations methods. The best adaption of travel times is observed by the nonlinear algorithm in combination with the 3D-model (P- and S-waves).

low velocities of the basins. The NS section reaches from the Bohemian Massif across the Eastern Alps to the Styrian Basin, again marked by lower velocities. This section also includes the transition from the European plate in the North, to the Pannonian fragment in the South. This lithospheric fragmentation has been revealed by the interpretation of the CELEBRATION 2000 and ALP 2002 data (Behm et al., 2007, Brückl et al, 2006; Brückl et al., 2007) and is closely related to the lateral extrusion process.

4.4 Station corrections

Station corrections can improve the accuracy of travel-time calculations in case of near-surface deviations of seismic velocities from the applied velocity model. We estimated station corrections to the 3D-velocity model by averaging the station residuals calculated by NonLinLoc. The permanent observatory CONA was chosen as the reference station. These station corrections are plotted and contoured in Figure 6. The known
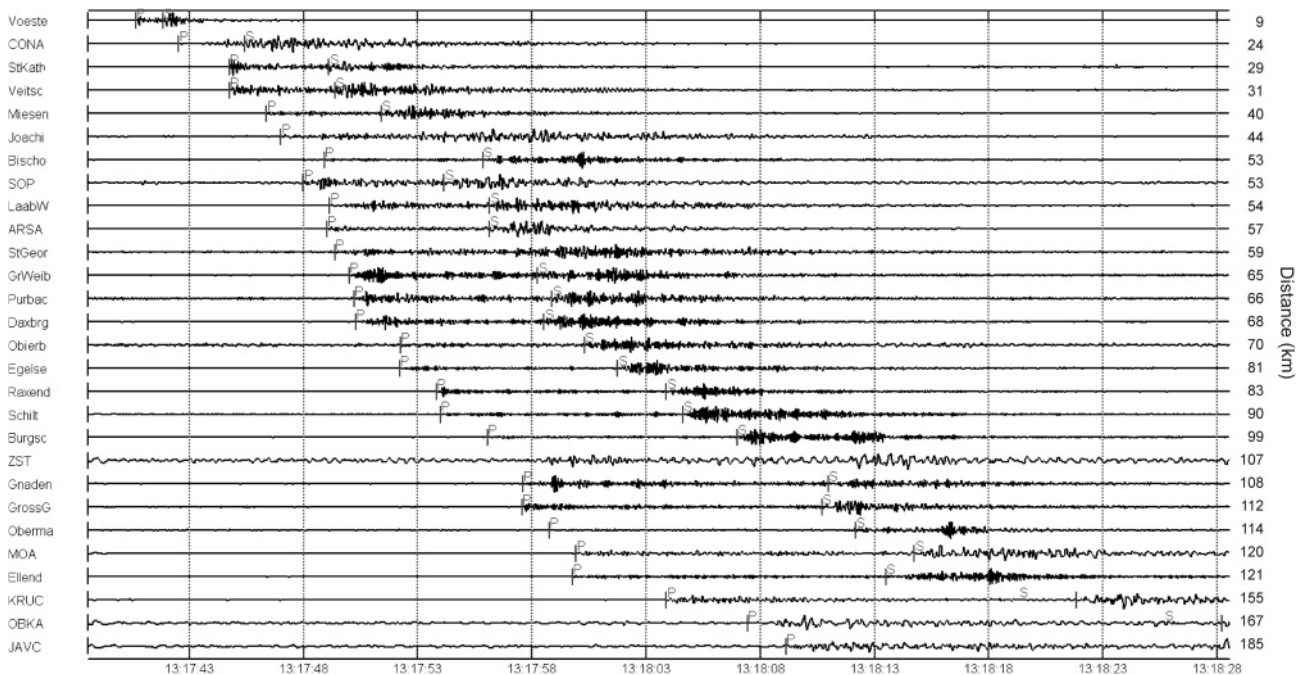
Figure 7: Example B of seismic data recorded at the Z-component and sorted by the epicentre distance from the bulletin. The magnitude Ml = 2.2 event occurred on 2006 04 15 13:17:38 and was located from ZAMG to be in the west of Neunkirchen (Fig. 2). The data were processed with frequency band-pass filter (1 – 12 Hz) and span a period of 50 seconds.
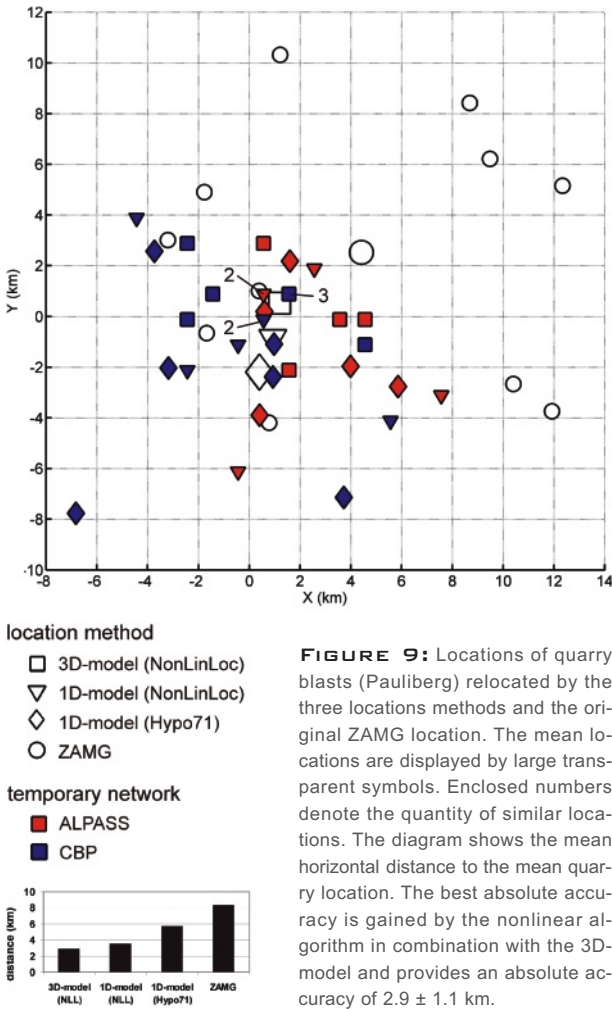
Figure 9: Locations of quarry blasts (Pauliberg) relocated by the three locations methods and the original ZAMG location. The mean locations are displayed by large transparent symbols. Enclosed numbers denote the quantity of similar locations. The diagram shows the mean horizontal distance to the mean quarry location. The best absolute accuracy is gained by the nonlinear algorithm in combination with the 3D-model and provides an absolute accuracy of 2.9 ± 1.1 km.

high value of ~ 1 s for the permanent station JAVC (Lenhardt, pers. comm.) is also evident from our data and not considered in the following. The station corrections range from -0.20 to +0.83 s and are correlated spatially over a distance of about 50 km. This result could be interpreted as an indication that an improvement of the 3D velocity model should be attempted. Husen et al., (2003) emphasize that station corrections are only meaningful if more than 10 observations per station exist. Since the available observations per station are indeed very low and highly variable (2 – 50), we relocated all events in this study without applying the station corrections.

5. Evaluation of location methods

In the following, we frequently refer to the routine locations supplied by ZAMG, which are based only on the recordings from the permanent observatories. The events were located using the global standard 1D-model IASPEI 1991 in combination with the dbloc2 module of the Antelope Software. Travel-times are picked including a weighting scheme. Residuals are listed, but station corrections are not used (Lenhardt, pers. comm.).

We compare the performance of the three different methods we applied for hypocentre location: the standard earthquake location routine Hypo71 with a constant 1D model (a), the probabilistic nonlinear earthquake location routine NonLinLoc with

a 1D- (b), and a 3D-velocity model (c). We selected four events located in or near the upper Mürz-Valley and the VB to evaluate these methods (for locations, see Fig. 2). The four datasets were selected on the basis of their data quality and the number of observations (P- and S-waves). One example is shown in Figure 7. Focal coordinates for the selected earthquakes depend considerably on the location method. The mean relative differences from all epicentre locations between each location method are listed in Table 1. The location routine Non LinLoc with the 3D model performs best.

5.1 Residual travel-times

The internal accuracy of the different location methods may be assessed by the travel-time residuals. RMS errors for travel-time residuals resulting from the three location methods and the ZAMG locations are shown in Figure 8 for each of the four events. The lowest travel-time residuals are obtained by the NonLinLoc algorithm with the 3D-model. For this method, the mean RMS error is 0.34 s (VAR = 0.116 s^2). The classification of the 182 P and S travel-times used for the location of these four earthquakes suggests a travel time error of ~0.25 s (VAR ~ 0.062s^2). These travel-time errors are one source for the travel-time residuals obtained by the location algorithm. Another source is the velocity model. Behm (2006) analysed the residuals of the travel-times used for the generation of the 3D P-wave velocity model we use in our area of interest. He estimated the RMS error as 0.26 s (VAR = 0.068 s^2), which can mainly be attributed to inaccuracies of the velocity field. From these figures we conclude that the contributions of the travel-time errors and the errors in the velocity model to the travel-time residuals obtained by the location algorithm are of similar magnitude.

5.2 Location of quarry blasts

Quarry blasts with known locations offer the possibility to assess the absolute accuracy of hypocentre locations. The quarry Pauliberg is located 26 km south of Wiener Neustadt (Fig. 2). Its location is representative of the central part of the study area. We used recordings from 11 blasts at the quarry Pauliberg and tested the three location methods described above. The geographic coordinates of the blasts were derived from aerial photographs and maps.

Figure 9 shows the individual and average locations of the quarry blasts calculated by the different methods and as a reference, the routine locations by ZAMG. The diagram shows the resulting mean horizontal and vertical distance to the actual position of the blasts in the quarry. NonLinLoc using the 3D velocity models performs best. A location error of ~3 km in horizontal and vertical direction can be derived from these results. No significant differences in the absolute accuracy between the two temporary networks ALPASS and CBP were observed, but azimuth-dependent deviations due to the different station geometry could be seen.
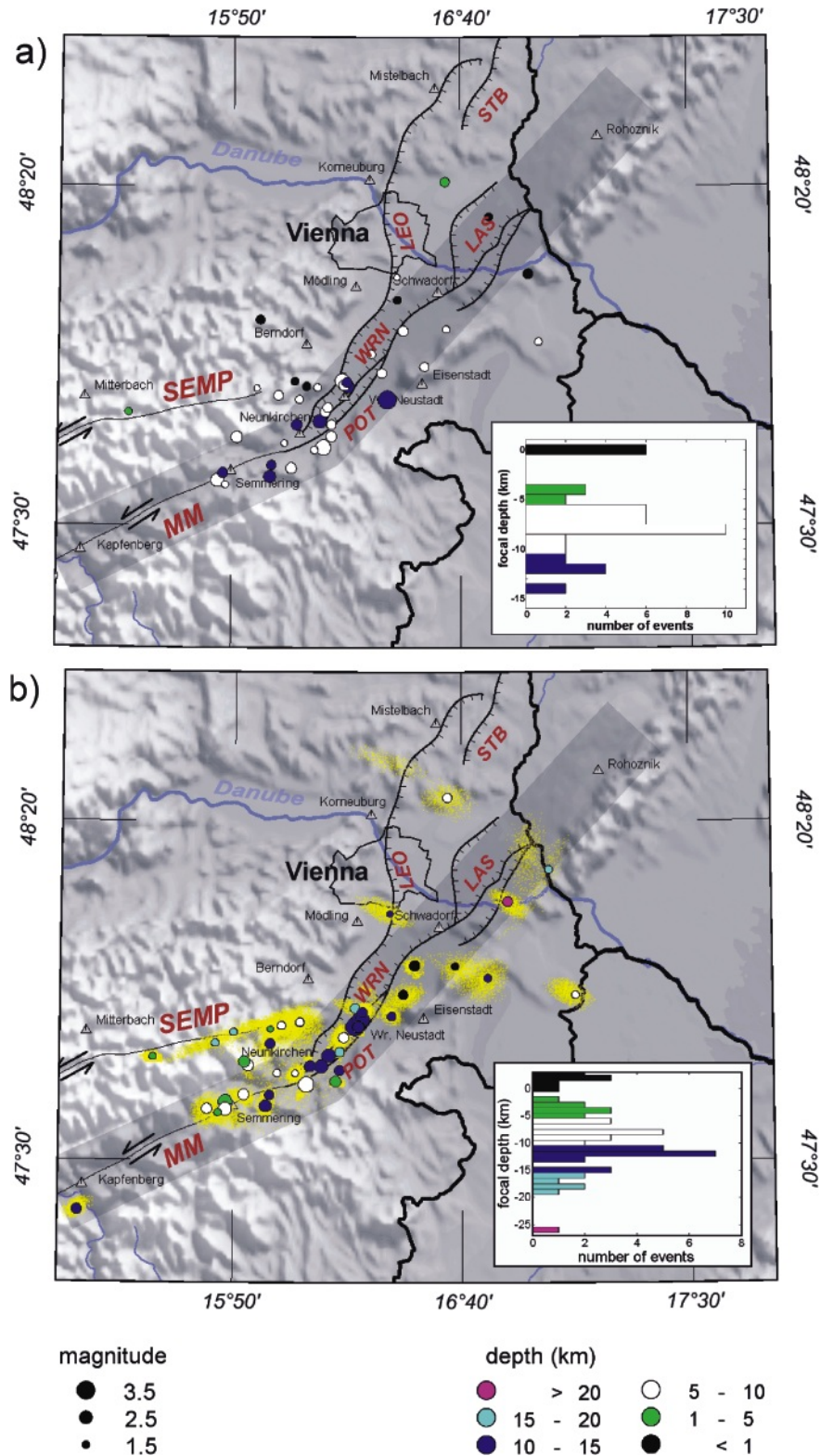
6. Seismicity and fault pattern

The evaluation of the location methods in the previous sec-

tion suggests that the probabilistic nonlinear earthquake location routine NonLin Loc (Lomax et al., 2000) in combination with the 3D velocity model performs best. Therefore, we concentrate on the locations calculated by this method (Tab. 2). We compare these results with the routine locations supplied by ZAMG on the basis of the few permanent stations in this area and discuss the potential of the data from the temporary network for an improved seismotectonic interpretation.

Figure 10 shows the major faults in our target area (after Kröll and Wessely, 1993; Linzer et al., 2002; Wessely, 2006) superimposed on a DTM, together with the epicentres located by ZAMG (Fig. 10a) and the new epicentres listed in Table 2 (Fig. 10b). The location of the faults in the Vienna Basin corresponds to fault heaves in the pre-Miocene basement (Kröll and Wessely, 1995; Wessely, 2006). Histograms of the focal depth obtained by the two methods and the PDF calculated by NonLinLoc are also shown. Large-scale structures are the Mur-Mürz and Salzach-Ennstal-Mariazell-Puchberg (SEMP) strike-slip faults and the Vienna Basin Transfer (VBT) fault, which comprises the Pottendorf fault, and the Wiener Neustadt and Lassee fault. The Leopoldsdorf and Steinberg fault delimit the Vienna Basin to the west.

The concentration of earthquakes around the Mur-Mürz and the southern Vienna Basin near Semmering, Neunkirchen, and Wiener Neustadt (for locations, see Fig. 10a) is well-known (e.g. NEIC catalogue, or earthquakes in Austria since 1200, ZAMG). The routine locations of the

earthquakes considered in this study group in the southern VB, ,but do not show any linear alignment. Thus, the correlation of these epicentres with the local faults (e.g. Pottendorf fault, SEMP) remains speculative. The new locations derived from the temporary networks and the 3D velocity model cluster around mapped faults and show pronounced fault-parallel linear alignments (Fig. 10b). The most significant linear align-

FIGURE 10: The major faults in our target area (after Kröll and Wessely, 1993; Linzer et al., 2002; Wessely, 2006) superimposed on a DTM, together with the epicentres (circles) located by ZAMG (a) and located by NonLinLoc in combination with the 3D velocity model and the additional data from the temporary networks (b). Histograms of the focal depth (see insets) obtained by the two methods and the PDF (yellow point clouds) calculated by NonLinLoc are also shown. LAS (Lassee fault), LEO (Leopoldsdorf fault), MM (Mur-Mürz fault), POT (Pottendorf fault), SEMP (Salzach-Ennstal-Mariazell-Puchberg fault), STB (Steinberg fault), WRN (Wiener Neustadt fault).

ment of epicentres is trending from SW (Semmering) to NE (Wiener Neustadt). These epicentres are well clustered and correlate with the Pottendorf and Wiener Neustadt faults sys-tems. The continuation of the SEMP towards the VB is also imaged by the new epicentres of low magnitude events. Figure 11 shows a crustal cross section from SW to NE along

			Original locations (ZAMG)				Relocations (NonLinLoc, 3D-model)			
Origin date & time		Ml	Sec.	X (m)	Y (m)	D (km)	Sec.	X (m)	Y (m)	D (km)
04.06.2005	03:11	1,9	25,26	589672	5288941	8	24,78	591500	5286000	12
06.06.2005	02:09	1,2	58,58	569241	5298543	6	58,36	572500	5297000	3
10.06.2005	16:45	2,0	41,63	608730	5314893	7	40,26	611500	5315000	0
13.06.2005	08:37	1,9	36,14	603199	5303229	7	36,29	595500	5303000	16
06.07.2005	18:47	1,2	52,88	606824	5329478	6	52,74	604500	5329000	11
11.07.2005	23:53	2,1	47,39	578905	5276857	10	47,08	565500	5279000	9
25.07.2005	03:06	3,5	58,57	604795	5296020	11	58,11	595500	5298000	13
25.07.2005	03:19	2,1	5,93	592977	5299787	8	5,39	596500	5298000	12
04.10.2005	14:34	1,6	16,81	580844	5295681	7	16,56	575500	5298000	8
03.11.2005	11:04	1,9	41,72	642528	5331234	0	42,85	636500	5333000	26
12.11.2005	05:26	1,8	31,12	619333	5355811	4	30,69	619500	5361000	9
18.11.2005	18:45	1,4	3,84	534274	5291594	4	3,84	540500	5289000	4
23.11.2005	20:57	2,1	19,67	580221	5288769	12	19,35	583500	5287000	11
28.12.2005	08:22	1,4	30,62	620490	5315539	9	29,48	622500	5315000	-1
03.02.2006	01:07	1,5	22,01	645729	5312742	6	21,30	655500	5308000	8
17.02.2006	09:16	1,5	30,23	607029	5323289	0	34,41	631500	5312000	11
02.03.2006	04:37	1,3	56,73	576937	5283667	6	56,31	579500	5285000	9
04.04.2006	20:23	1,9	12,11	593743	5300566	11	11,60	597500	5302000	12
11.04.2006	19:07	1,4	6,94	561016	5272107	6	7,09	558500	5274000	2
15.04.2006	13:17	2,2	39,13	563925	5285165	8	38,72	566500	5287000	10
16.05.2006	11:41	1,5	23,76	585729	5299030	6	24,67	557500	5293000	19
30.06.2006	17:55	2,4	8,67	593955	5299447	15	8,45	596500	5298000	16
01.07.2006	11:43	2,7	12,38	592411	5301001	8	12,16	597500	5300000	15
24.08.2006	13:29	1,5	5,44	579548	5300620	0	6,00	562500	5296000	18
29.08.2006	10:18	1,5	5,07	631483	5346504	0	3,21	647500	5342000	18
07.11.2006	15:39	1,8	2,96	614784	5305171	8	2,24	608500	5307000	-2
08.11.2006	21:16	1,5	29,87	508067	5243565	4	29,45	509500	5248000	-2
12.11.2006	19:26	2,3	22,44	508632	5244533	5	22,48	511500	5249000	3
25.11.2006	17:18	3,0	42,86	587562	5282694	8	43,28	582500	5282000	6
22.12.2006	07:55	1,8	13,75	573517	5277642	12	13,81	572500	5279000	12
22.12.2006	08:01	2,3	50,47	573128	5274492	14	49,72	571500	5276000	11
11.01.2007	01:32	1,7	30,91	600184	5308379	10	29,92	605500	5301000	15
05.02.2007	11:30	2,1	58,43	589707	5285706	8	58,31	590500	5283000	4
06.02.2007	13:36	1,7	16,35	569822	5317235	0	16,22	580500	5299000	8
26.02.2007	04:19	1,9	34,94	575140	5296682	7	34,65	572500	5293000	12
05.03.2007	16:11	2,0	31,92	560306	5275356	12	32,03	555500	5275000	8
22.03.2007	16:32	1,6	42,92	582747	5299287	0	43,41	580500	5299000	6
08.04.2007	20:32	2,3	27,51	507606	5243487	5	27,34	506500	5248000	-2
20.05.2007	07:28	2,0	59,49	514345	5246433	8	59,55	520500	5247000	11
02.07.2007	16:12	1,5	43,55	585150	5281903	8	43,67	574500	5285000	8
09.07.2007	10:19	2,6	52,55	586525	5289838	12	52,02	586500	5287000	15
16.07.2007	00:00	2,6	45,01	558862	5273252	9	43,95	560500	5275000	6
20.07.2007	06:20	2,0	23,84	587948	5292416	8	23,68	592500	5295000	10
20.07.2007	07:41	1,9	59,00	588641	5293649	8	58,39	591500	5291000	17

Table 2: Hypocentres (UTM33N) evaluated routinely by ZAMG (1D-model, permanent network) and relocated in this study by NonLinLoc, the implementation of a new 3D model for P-and S-waves, and data from permanent and temporary networks.

the MM fault and the VBT. The mapped focal depths belong to earthquakes located within the highlighted band in Figure 10. The new focal depths trend to get deeper towards NE, whereas the routine locations lack a trend. Only very few earthquakes were observed in the central part of the Vienna Basin. Several of these events are very shallow and some may be quarry blasts. Another event near the Lassee fault has a focal depth >20 km. These events need further inspections of data quality and we do not include them in our preliminary correlation with known faults.

7. Discussion and outlook

Data from temporary (ALPASS and CBP) and permanent seismic networks were used to improve earthquake location for seismo-tectonic interpretation in the Vienna Basin area. We tested three absolute location methods in order to analyse the influence of the algorithms and velocity models on the location accuracy: the linearized algorithm of Hypo71 (Lee and Lahr, 1975) in combination with a local 1D velocity model, and the earthquake location method NonLinLoc (Lomax et al., 2000), in combination with either a 1D velocity model or a 3D velocity model derived from CELEBRATION 2000 and ALP 2002 data (Behm et al., 2007; Behm, 2009). The 1D velocity model represents an average of the 3D model over the investigation area. The probabilistic nonlinear algorithm implemented in NonLinLoc together with the 3D velocity model for P- and S-waves turned out to be the most consistent and accurate method. The new epicentre locations of the 44 earthquakes investigated in this study differ considerably from the routine location of ZAMG (Table 2, Figs. 10, 11).

The assessment of the absolute accuracy provided by different hypocentre location methods is a complex task due to the unknown absolute earthquake location. Further difficulties arise from the accuracy of the velocity model, the network geometry, and the accuracy, number, and type of travel-times. As a first criterion we considered the RMS error for travel-time residuals of four selected events with high data quality. The best data fit was provided by the nonlinear algorithm (NonLinLoc) in combination with the 3D-model for P- and S-waves. A second criterion was the performance of the different methods at the location of quarry blasts (Pauliberg) with known locations. Again the nonlinear location routine NonLinLoc in combination with the 3D seismic velocity models performed best. These results led to the decision to use only this method for the relocation all 44 earthquakes.

A quantitative measure of the reliability of the earthquake locations is the density scatter plot for the PDF values, as shown in Figure 10b. An improved alignment of relocated hypocentres and the stacked PDF scatter plots to known active faults may be regarded as an a posteriori criterion for the assessment of the accuracy of location methods, the implemented seismic velocity model and the number and geometry of seismic stations. The comparison of the routine locations of ZAMG and the relocations with NonLinLoc and the 3D seismic velocity models (Figs. 10, 11) shows clearly that the relocations are
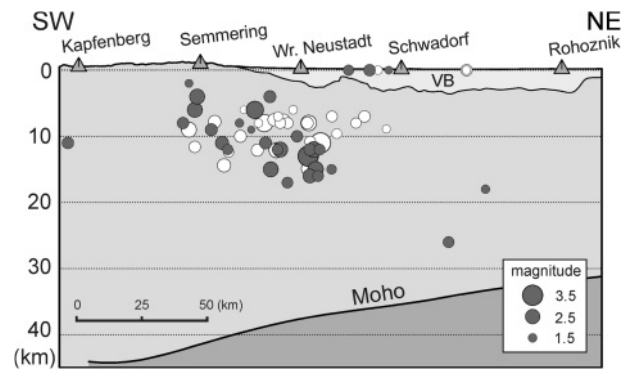
Figure 11: Crustal cross section of hypocentres along the MM fault and the VBT (for location, see Fig. 10) with the Vienna Basin (Miocene) (after Wessely, 1993) and the Moho (after Behm et al., 2007). In contrast to the routine locations (white) the new hypocentres (dark grey) display focal depths which get deeper towards NE.

sufficiently accurate to allow for a correlation with known active faults and a seismotectonic interpretation. Significant correlations are found with the Pottendorf and Wiener Neustadt faults systems. Further, the continuation of the Salzach-Ennstal-Mariazell-Puchberg fault towards the VB has been imaged clearly by epicentres. The trend of increasing focal depth from SW to NE in the southern Vienna Basin (Fig. 11) seems also geologically reasonable.

We classify our results as encouraging, but preliminary. The ongoing project ALPAACT (Seismological and geodetic monitoring of ALpine-PAnnonian ACtive Tectonics, http://info.tuwien.ac.at/geophysik/research/alpdynamics.htm) continues the efforts of this study over a longer period. The existing 3D velocity model will be further improved by reducing systematic errors (e.g. near-surface corrections) to enable network independent improved earthquake location. Further, a quasi-permanent (> 4 years) densification of the observatory network is in progress. Selections of these new stations take advantage of the experience gained during ALPASS and CBP. In collaboration with ZAMG the improved and expanded 3D velocity model will be implemented into the routine location of earthquakes in the whole area of Austria.

References

Aric, K. and Gutdeutsch, R., 1981. Seismotectonic and refraction seismic investigation in the border region between the Eastern Alps and the Pannonian Basin. Pure and Applied Geophysics., 119, 1125–1133.

Behm, M., 2006. Accuracy and resolution of a 3D seismic model of the Eastern Alps. Ph.D. thesis, Vienna University of Technology, Vienna.

Behm, M., E. Brückl, W. Chwatal, and H. Thybo, 2007. Application of stacking techniques to 3D wide-angle reflection and refraction seismic data of the Eastern Alps. Geophysical Journal International, 170 (1), 275-298, doi: 10.1111/j.1365-246X. 2007.03393.x.

Behm, M., 2009. 3-D modelling of the crustal S-wave velocity structure from active source data: application to the Eastern Alps and the Bohemian Massif. Geophysical Journal International, 179(1), 265-278, doi:10.1111/j.1365-246X.2009.04259.x.

Brückl, E., T. Bodoky, E. Hegedues, P. Hrubcová, A. Gosar, M. Grad, A. Guterch, Z. Hajnal, G.R. Keller, A. Špičák, F. Sumanovac, H. Thybo, F. Weber, and ALP 2002 Working Group (2003). ALP 2002 Seismic Experiment, Studia geophysica geodaetica, Academy of Sciences of the Czech Republic, Volume 47. ISSN 0039-3169, 671-679.

Brückl, E., Lippitsch, R., Mitterbauer, U., and ALPASS working groups, 2008. Alpass - Teleseismic tomography of the Eastern Alps. Oral Presentation at Pangeo 2008, 22-25 September 2008. Journal of Alpine Geology, 49, 16, ISSN 1563-0846.

Decker, K., 1996. Miocene tectonics at the Alpine–Carpathian junction and the evolution of the Vienna Basin. Mitteilungen der Gesellschaft der Geologie und Bergbaustudenten Österreich, 41, 33–44.

Decker, K. and Peresson, H., 1998. Miocene to present-day tectonics of the Vienna Basin transform fault. In: Links Between the Alps and the Carparthians, XVI Congress of the Carparthian–Balkan Geological Association, 33–36. Geologische Bundesanstalt, Vienna.

Decker, K., Peresson, H., and Hinsch, R., 2005. Active tectonics and Quaternary basin formation along the Vienna Basin Transform fault. Quaternary Science Reviews, 24, 307-322.

Decker, K., Gangl, G. and Kandler, M. 2006. The earthquake of Carnuntum in the 4th century AD - archaeologic results, seismologic scenario and seismo-tectonic implications for the Vienna Basin Fault, Austria. Journal of Seismology, 10(4), 479-495, doi: 10.1007/s10950-006-9032-0.

Decker, K., and Burmester, G. 2008. Stress orientations and active fault kinematics of the Vienna Basin Fault System, Austria. 3rd World Stress Map Conference, 15-17 October 2008, Potsdam, 110.

Deichmann, N., 1987. Focal depths of earthquakes in northern Switzerland, Annales Geophysicae, 5B, 395– 402.

Gangl, G., 1975. Seismotektonische Untersuchungen am Alpenostrand. Mitteilungen der Geologischen Gesellschaft in Wien, 1973-1974(66-67): 33-48.

Geiger, L., 1912. Probability method for the determination of earthquake epicenters from the arrival time only (translated from Geiger's 1910 German article). Bulletin of St. Louis University, 8(1), 56-71.

Grenerczy, G., Kenyeres, A. and Fejes, I., 2000. Present crustal movement and strain distribution in Central Europe inferred from GPS measurements. Journal of Geophysical Research, 105 (B9), 21835–21846.

Grenerczy, G., 2002a. Tectonic processes in the Eurasian–African plate boundary zone revealed by space geodesy. In: S. Stein and J. T. Freymueller (eds), Plate Boundary Zones. Geodynamics Series, 30, 67–86, American Geophysical Union.

Grenerczy, G., 2002b. Towards a dense intraplate velocity map for Central Europe. Reports on Geodesy, 1 (61).

Guterch, A., M. Grad, G. R. Keller, K. Posgay, J. Vozar, A. Špičák, E. Brueckl, Z. Hajnal, H. Thybo, O. Selvi, and CELEBRATION 2000 Experiment Team (2003). CELEBRATION 2000 Seismic Experiment, Stud. Geophys. Geod., 47, pp. 659-669.

Gutdeutsch, R., Mayer, I., Hammerl, Ch. and Vocelka, K., 1987. Erdbeben als historisches Ereignis – Die Rekonstruktion des niederösterreichischen Erdbebens von 1950. Berlin - Heidelberg – Wien (Springer) 1987.

Gutdeutsch, R. and Aric, K., 1988. Seismicity and neotectonics of the East Alpine–Carpathian and Pannonian Area. In: L. H. Royden and F. Horvath (eds), The Pannonian Basin: a Study in Basin Evolution. AAPG Memoir, 45, 183–194.

Hammerl, C. and Lenhardt, W. 1997. Erdbeben in Österreich, Leykam Verlag Wien.

Haslinger, C., Krauss, S. and Stangl, G., 2007. The Intra-Plate Velocities of GPS Permanent Stations of the Eastern Alps. Vermessung und Geoinformation, 2, 66-72.

Hinsch, R. and Decker, K., 2003. 3-D mapping of segmented active faults in the Vienna Basin from integrated geophysical, geomorphological and geological data: building up an active fault database, EGS-AGU-EUG Joint Assembly, Nice. Geophysical Research Abstracts, Vol. 5. European Geophysical Society, pp. 10272.

Hinsch, R., Decker, K. and Wagreich, M., 2005a. A short review of Environmental Tectonics of the Vienna Basin and the Rhine Graben area. Austrian Journal of Earth Sciences, 97, 6-15.

Hinsch, R., Decker, K. and Wagreich, M., 2005b. 3-D mapping of segmented active faults in the southern Vienna Basin. Quaternary Science Reviews, 24, 321-336.

Houseman, G., Stuart, G., Hegedüs, E., Brückl, E., Radovanovic, S., Brisbourne, A., Lorinczi, P., Dando, B., Kovacs, A. and Hausmann, H., 2008. Preliminary results from the Carpathian Basins Project: an investigation of the seismic structure of the lithosphere in the Pannonian and Vienna Basins. Oral Presentation at EGU, General Assembly, Vienna, Austria, 13-18 April 2008. Geophysical Research Abstracts, Vol. 10, EGU 2008-A-05716, 2008, SRef-ID: 1607-7962/gra/EGU2008-A-05716.

Höggerl, N., 1989. Rezente Höhenänderungen in Österreich abgeleitet aus Präzisionsnivellement-Messungen, Österreichische Beiträge zu Meteorologie und Geophysik, 2, 161-173.

Husen, S., Kissling, E., Deichmann, N., Wiemer, S., Giardini, D. and Baer, M., 2003. Probabilistic earthquake location in complex three-dimensional velocity models: Application to Switzerland. Journal of Geophysical Research 108 (B2): 2077. doi: 10.1029/2002JB00177.

Kissling, E., W.L. Ellsworth, D. Eberhart-Phillips, and U. Kradolfer 1994. Initial reference models in local earthquake tomography, Journal of Geophysical Research, 99, 19635-19646.

Klein, F. W., 2002. User's guide to HYPOINVERSE-2000, a Fortran program to solve for earthquake locations and magnitudes, U.S. Geological Survey, Open-File Report 02-171, 123 pp.

Kröll, A. and Wessely, G., 1993. Karten über den Untergrund des Wiener Beckens uns der angrenzenden Gebiete, Geologische Themenkarten der Republik Österreich, Maßstab 1:200.000, Geologische Bundesanstalt, Wien.

Lahr, J. C., 1999. HYPOELLIPSE: a computer program for determining local earthquake hypocentral parameters, magnitude, and first-motion pattern (Y2K compliant version), U.S. Geological Survey, Open-File Report, 99-23, 123 pp.

Lee, W.H.K. Lahr, J.C., 1975. A computer program for determining local earthquake hypocenter, magnitude, and first motion pattern of local earthquakes, U.S. Geological Survey, Open-File Report, 75–311.

Lenahrdt, W.A., Švancara, J., Melichar, P., Pazdirkova, J., Havir, J. and Sykorova, Z. 2007. Seismic activity of the Alpine-Carpathian-Bohemian Massif region with regard to geological and potential field data. Geologica Carpathica, 58, 397-412.

Linzer, H.-G., Moser, F., Nemes, F., Ratschbacher, L. and Sperner, B., 1997. Build-up and dismembering of a classical fold-thrust belt: from non-cylindircal stacking to lateral extrusion in the eastern Northern Calcareous Alps. Tectonophysics, 272, 97-142.

Linzer, H.-G., K. Decker, H. Pereson, R. Dell'Mour and W. Frisch 2002. Balancing lateral orogenic float of the Eastern Alps, Tectonophysics, 354, 211-237.

Lomax, A., Virieux, J.,Volant P. and Berge, C., 2000. Probabilistic earthquake location in 3D and layered models: Introduction of a Metropolis-Gibbs method and comparison with linear locations, in Advances in Seismic Event Location Thurber, C. H., and N. Rabinowitz (eds.), Kluwer, Amsterdam, 101-134.

Marsch, F., Wessely, G. and Sackmaier, W., 1990. Borehole-breakouts as geological indications of crustal tension in the Vienna Basin. In: Mechanics of Joined and Faulted Rock (P. Rossmanith, ed.), pp. 113–120. Balkema, Rotterdam.

Mertl, S. and Hausmann, H., 2009. Seismon - a flexible seismic processing software. Poster Presentation at EGU, General Assembly, Vienna, Austria, 19-24 April 2009. Geophysical Research Abstracts, Vol. 11, EGU2009-4266.

Oberhauser, R., 1980. Der Geologische Aufbau Österreichs. 699 pp, Springer, Wien, New York.

Peresson, H. and Decker, K., 1997. The Tertiary dynamics of the Northern Eastern Alps (Austria): Changing paleostresses in a collisional plate boundary. Tectonophysics, 272, 125-157.

Podvin, P. and Lecomte, I., 1991. Finite difference computation of traveltimes in very contrasted velocity models: a massively parallel approach and its associated tools., Geophysical Journal International, 105, 271-284.

Pujol, J., 1995. Application of the JHD technique to the Loma Prieta, California, mainshock-aftershock sequence and implications for earthquake location. Bulletin of the Seismological Society of America (February 1995), 85(1), 129-150.

Ratschbacher, L., Frisch, L.W., Linzer, H.G., and Merle, O., 1991. Lateral extrusion in the Eastern Alps, Part 2.: Structural analysis, Tectonics, 10, 2, 257-271.

Reinecker, J. and Lenhardt, W.A., 1999. Present-day stress field and deformation in eastern Austria. International Journal of Earth Sciences, 88,532-530.

Rietbrock, A. and Scherbaum, F. 1998. The GIANT analysis system, Seismological Research Letters, Electronic Seismologist, 69 (1), 40-45.

Royden, L.H. 1993. Evolution of retreating subduction boundaries formed during continental collision, Tectonics, 12 (3), 629-638.

Schmid, S., Fügenschuh, B., Kissling, E. and Schuster, R., 2004. Tectonic map and overall architecture of the Alpine orogen. Eclogae Geologicae Helvetiae, 97(1), 93-117,doi: 10.1007/s00015-004-1113-x.

SED, 2000. Schweizerischer Erdbebendienst, Regional Moment Tensor Catalog 2000, Available http://www.seismo.ethz.ch/moment_tensor/2000/homepage.html (June 2009).

Senftl, E. and Exner, C., 1973. Rezente Hebung der Hohen Tauern und geologische Interpretation. Verhandlungen der Geologischen Bundesversuchsanstalt, 1973/2. 209–234.

Tarantola, A. and Valette, B., 1982. Inverse problems = quest for information. Journal of Geophysics, 50, 159-170.

Vyskocil, P., 1994. Map of annual velocities (regional trends) of vertical surface movements on the territory of a part of Central Europe. XXVII General Assembly of the European Geophysical Society (EGS), Geodetic and Geodinamic Programmes of the CEI, – Nice, France, 21-26 April 2002, 8 p.

Waldhauser, F., and Ellsworth, W.L., 2000. A double-difference earthquake location algorithm: method and application to the northern Hayward fault, California, Bulletin of the Seismological Society of America, 90 (6), 1353–1368.

Wessely, G., 1987. Mesozoic and Tertiary evolution of the Alpine-Carpathian foreland in eastern Austria. Tectonophysics 137, 45-59.

Wessely, G., 2006. Geologie der österreichischen Bundesländer – Niederösterreich. Wien, Verhandlungen der Geologischen Bundesversuchsanstalt, 416 pp.

Zimmer, W., Wessely, G., 1996. Exploration results in thrust and subthrust complexes in the Alps and below the Vienna Basin in Austria. In: Wessely G, and Liebl W. (eds). Oil and gas in Alpidic thrustbelts and basins of Central and Eastern Europe. EAGE Special Publications, 5, 81–107.

Helmut HAUSMANN[1)*)], Stefan HOYER[2)], Bernd SCHURR[2)3)], Ewald BRÜCKL[1)], Gregory HOUSEMAN[4)] & G. STUART[4)]

[1)] Institute of Geodesy and Geophysics, Vienna University of Technology, Gusshausstrasse 27-29/1282, A-1040 Vienna, Austria;

[2)] Department of Meteorology und Geophysics, University of Vienna, Althanstrasse 14, A-1090 Vienna, Austria;

[3)] Department of Geodynamics, Helmholtz-Zentrum Potsdam, Deutsches GeoForschungsZentrum GFZ, Telegrafenberg, C 223, D-14473 Potsdam, Germany;

[4)] Faculty of Earth and Environment, University of Leeds, Leeds, LS2 9JT, UK;

[*)] Corresponding author, hausmann@mail.zserv.tuwien.ac.at